Time dependence of the cosmological astrophysical background of gravitational waves.

E Howell, D Coward, R Burman and D Blair
School of Physics, University of Western Australia (M013),
Crawley WA 6009, Australia

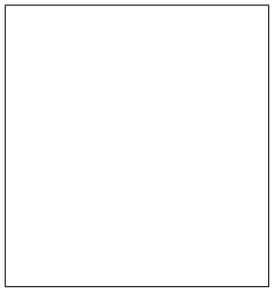

Stochastic background signals from throughout the universe are normally considered to be statistically stationary and time independent. We point out that the astrophysical cosmological background of gravitational wave bursts has a unique and strong time dependence. This time dependance arises because of the expansion and structure of the universe. During the observation time which is assumed to extend from seconds to years, the spectrum evolves towards the blue. Over time the background is first dominated by frequent distant and red shifted events, while after long observation times it is dominated by rare nearby events. We introduce the concept of a probability horizon, and show that the horizon velocity ranges from extreme superluminal velocity to modest velocity during the observation period. We have developed techniques to model all the gravitational wave burst events in the universe at a rate faster than real time. This allows us to examine the signals in detail. The background spectrum converges over time to a stable spectrum, which arises through the interplay of star formation and cosmology. Issues of detectability are discussed in the context of advanced laser interferometer gravitational wave detectors.

PACS numbers: 04.30.Db, 04.80.Nn, 97.60.Jd, 98.70.Vc, 98.80.-k

1 Introduction

Three long-baseline laser interferometric gravitational wave (GW) detectors have been built, or are near completion. The US LIGO (Laser Interferometer Gravitational-wave Observatory) has completed several science runs; it consists of two 4-km arm detectors situated at Hanford, Washington, and Livingston, Louisiana. The Italian/French VIRGO collaboration is completing a 3-km baseline instrument at Cascina, near Pisa [a]. These instruments are unlikely to be sensi-

[a] For further information on these projects visit:
LIGO—http://www.ligo.caltech.edu/

tive enough to detect many of the proposed astrophysical GW sources over practical observation times; however, the next generation of interferometric detectors, planned to go online late this decade, should be sensitive to a host of sources. These 'Advanced' interferometers could revolutionize our understanding of the Universe, providing a new window to the cosmos not accessible by conventional astronomy.

The strongest GW sources, in the band most sensitive to Advanced interferometers, include coalescing compact binaries [8] [17], core-collapse supernovae [14] [10], and dynamic instabilities of post-collapse compact remnants [9]. Transient GW emissions, associated with core-collapse supernovae (SNe), must occur frequently throughout the Universe, and their combined signal will form a stochastic GW background, potentially detectable by Advanced interferometric detectors.

Despite the uncertainty in the neutron star (NS) formation rate and in the GW emissions resulting from core-collapse SNe, estimates of the spectral properties of a stochastic GW background from such sources have been presented by a number of authors. Ferrari, Matarrese and Schneider[7] calculated the stochastic background from a cosmological population of young, hot, rapidly rotating neutron stars that radiate GW energy through the r-mode instability. Coward, Burman and Blair [4] investigated the GW background from NS birth by employing a representative sample of axisymmetric rotational core-collapse models developed by Zwerger and Müller [22]. Using the Einstein-de Sitter cosmology and a star formation rate (SFR) model from Madau, Pozetti and Dickenson [16], they calculated the GW spectrum from sources in the range $0-5$ of redshift z by convolving the differential rate of NS formation with a single-source GW fluence (time-integrated flux), integrated over z. They showed that the background spectrum retained a dependence on the single-source emission spectrum, and calculated a duty cycle of order unity. Howell [12] updated this work using simulated core-collapse GW waveforms, modelled with general relativity by Dimmelmeier, Font and Müller [6](hereafter DFM). They found that the GW background from NS formation is unlikely to be detected by Advanced LIGO detectors. However, preliminary results [13] show that the background will be considerably enhanced by dynamic post-collapse instabilities (bar modes) if they are a frequent feature of NS birth.

Coward, Burman and Blair [5](hereafter CBB) developed a procedure for simulating the GW background from neutron star formation over cosmological distances. Assuming the SFR model of Madau, Della Valle and Panagia [15] and the Einstein-de Sitter cosmology, they derived the probability density function, $P(z)$, for NS births as a function of z. They found the background GW strain to be dominated by sources at $z \approx 2-3$ and that the distribution of GW amplitudes is highly skewed, with skewness related to the low-z distribution of sources.

In this study, we extend this simulation procedure to investigate the temporal evolution of a simulated GW spectrum with a source rate history that peaks at a relatively high redshift. We use a short-duration, nearly monochromatic waveform, with a characteristic frequency of 1 kHz, allowing us to investigate the temporal evolution of the spectra without the added complications arising from using more complex waveforms.

The paper is organized as follows: In Section 2 we discuss the evolution of the NS birth rate throughout the universe using a SFR model that peaks at particularly high redshift. We describe the simulation procedure in Section 3, define a probability event horizon in Section 4 and present our results in Section 5. In section 6 we discuss the main features of our results.

2 Neutron star birth rate evolution

The progenitors of compact remnants are relatively short-lived stars with masses greater than 8–10 $M_\odot$ and lifetimes of the order of tens of Myr; hence their formation rate will closely track the SFR [21]. But uncertainties in determining the SFR history from co-moving luminosity densities

VIRGO—http://www.virgo.infn.it/

— particularly the allowance to be made for dust extinction [19] — have led to several alternative models for the cosmic SFR history being proposed.

In a different approach, Springel and Hernquist [20](hereafter SH) developed a simulation of the SFR history in a 'flat-Λ' cosmology (a spatially flat cosmology with a cosmological constant). Their model shows a peak at $z \approx 5 - 6$, significantly higher than in most of the observation-based models. It is supported by data from the Wilkinson Microwave Anisotropy Probe [1] [2] that suggests that reionization occurred at $z > 10$. Because of the uncertainty in the SFR at high z, we adopt the SFR model of SH to highlight the effect of high-z SFR evolution on the spectral evolution of a stochastic background of GWs.

We use an analytical fit to the SH simulation developed by Hernquist and Springel [11], which includes a scaling related to the evolving expansion rate of the Universe, represented by the Hubble parameter $h(z) \equiv H(z)/H_0$. For a flat-Λ cosmology ($\Omega_{\rm m} + \Omega_\Lambda = 1$), we use $\Omega_{\rm m} = 0.3$ and $\Omega_\Lambda = 0.7$ for the $z = 0$ density parameters, and take $H_0 = 70$ km s^{-1} Mpc^{-1} for the Hubble parameter at the present epoch. With $\dot{\rho}_*$ donating the mass converted to stars per unit time and volume, the fit takes the form

$$\dot{\rho}_*[h(z)] = \dot{\rho}_{*[z=0]} \frac{h^{4/3}}{1 + \alpha(h^{2/3} - 1)^3 \exp(\beta h^{7/6})} \ , \qquad (1)$$

with $\dot{\rho}_{*[z=0]} = 0.013$ M$_\odot$ yr^{-1} Mpc^{-3}, $\alpha = 0.012$ and $\beta = 0.041$.

Assuming this SFR model and a NS formation rate density of 5×10^{-12} NS s^{-1} Mpc^{-3} in the nearby Universe, Howell *et al* [12] (their section 2) calculated the cumulative rate of NS birth, $R^{\rm NS}$, to be about 25 s^{-1} for sources in $z = 0 - 10$; these events are separated temporally by a mean interval $\tau = (R^{\rm NS})^{-1} = 40$ ms.

3 Simulating the GW spectrum

The GW emission from SN core collapse is highly uncertain. For example, earlier models (DFM) predicted that the maximum GW amplitude occurs at the time of core bounce; however, recent hydrodynamical simulations of Müller *et al* [18] suggest that the dominant contribution to the GW emission is not produced by stellar core bounce, but by neutrino convection behind the SN shock — this results in GW amplitudes an order of magnitude larger at ≈ 100 ms after the core bounce.

For illustrative purposes, we use here a highly simplified input waveform, $h(t)$ — a quasi-monochromatic damped sinusoid of characteristic rest-frame frequency 1 kHz and duration 10 ms, with a maximum dimensionless strain amplitude of 7×10^{-24} at a fiducial distance of 10 Mpc. The waveform duration is approximately that of strongest GW emission of a DFM Type I (regular collapse) waveform, corresponding roughly to the ringdown phase.

The amplitude and duration of the waveform are defined by the random variable z, generated from the probability density function $P(z)$:

$$P(z) = \frac{{\rm d}R^{\rm NS}/{\rm d}z}{\int_0^{10} ({\rm d}R^{\rm NS}/{\rm d}z)\,{\rm d}z} \ , \qquad (2)$$

(cf. CBB, Section 3) where ${\rm d}R^{\rm NS}/{\rm d}z$ is the differential rate of NS formation; $P(z){\rm d}z$ is the probability that an event occurred in the redshift shell z to $z + {\rm d}z$. As plotted in Figure 1, $P(z)$ shows that the most probable events occur at $z \approx 3 - 4$.

For a simulation of N events, the GW wave amplitude for each $h_{\rm i}(t)$, i $= 1, \ldots N$, is scaled inversely by the luminosity distance $d_{\rm L}(z)$ and the signal duration is time-dilated by the factor $(1 + z)$. As the temporal distribution of events in our frame is a stochastic, memory-less point process, the mean time interval between successive events, τ, will follow an exponential

distribution. Successive waveforms are generated and combined to form a wave-train defined by the random variables z and τ. Because the signal durations are of order milliseconds, a high sampling rate of 16,384 Hz (2^{14} Hz) ensures that the sampled data stream is free from any discontinuities that would produce spurious high-frequency components in the spectrum.

Time slices, corresponding to 1 s of real-time data, are simulated and Fast Fourier Transforms (FFTs) of length 2048 are calculated using a Hanning window. Individual spectra, $S_{\rm n}(f)$ in Hz^{-1}, of these time slices are accumulated at a rate ≈ 4 times 'real' time for our 2.8-GHz processor. Successive spectra are averaged to yield a power spectrum defined as

$$S(f) = \sum_n S_{\rm n}(f)/n \ = |h(f)|^2, \tag{3}$$

where $h(f)$, in $\mathrm{Hz}^{-1/2}$, is the GW background strain.

This procedure allows us to study the temporal evolution for different simulation lengths of data, corresponding to observations of different durations.

4 The Probability Event horizon

For any astronomical detector and source type, one can define a 'detectability horizon' centred on the detector and encompassing the volume in which such events are potentially detectable; the horizon distance is determined by the flux limit of the detector and the source flux. A second horizon, defined by the minimum distance for at least one event to occur over some observation time, with probability above some selected threshold, can also be defined. We call this the 'probability event horizon' (PEH) (see Coward and Burman[3]). It describes how an observer and all potentially detectable cosmological events of a particular type are related via a probability event distribution encompassing all such events. The evolution of the simulated GW spectrum depends on the PEH.

5 Results

Figure 2 shows the averaged GW power spectrum for a simulation of 30 million events – equivalent to 2 weeks of data for an event rate of $25\,\mathrm{s}^{-1}$ in our frame. For comparison, this figure also shows a power spectrum calculated by convolving a simulated single-source GW spectrum with the differential rate of source formation over the redshift range $0.002 < z < 10$, where $z = 0.002$ corresponds to about 10 Mpc. The ripples in the convolved spectrum are numerical noise. The amplitude of the power spectrum $|h(f)|^2 \approx 10^{-56}\ \mathrm{Hz}^{-1}$ is in correspondence with the background strain $h(f) \approx 10^{-28}\ \mathrm{Hz}^{-1/2}$, calculated for a GW background resulting from NS core-collapse using the waveforms of DFM[12].

The most prominent feature of the integrated spectrum is the broad peak at 200 – 250 Hz, resulting from the high rate of events in the redshift shell $4.0 > z > 3.5$, corresponding to the maximum of the differential event rate (Fig. 1). At frequencies greater than this there is a gently decreasing trend in power spectral density towards the rest-frame frequency of 1 kHz. The temporally simulated spectrum converges to the integrated convolved spectrum after about 8×10^5 events.

For a universal event rate of $25\,\mathrm{s}^{-1}$, the fastest spectral evolution occurs during the first seconds of observation time. This characteristic is dramatically highlighted in the supplementary animation, where there is an initial rapid increase in bandwidth from 550 Hz to 900 Hz for the first events, corresponding to sources in $z \approx 9$– 0.7. Figure 3 shows three frames from the movie at increasing times, illustrating the trend of increasing bandwidth as the number of events increases.

After this initial rapid spectral evolution, there is an intermediate period corresponding to $N = 10^2 - 10^4$ events. A "snapshot" of the spectrum from this period is shown in Figure 4. For data streams with temporal durations corresponding to $N \approx 300 - 400$, the rate of increase in bandwidth decreases because events outside the shell $0.2 < z < 0.9$ are less probable. The temporal evolution of the spectrum during this time is dominated by two components — a stable low-frequency peak at about 250 Hz, corresponding to the maximum of the differential source rate, and a non-stationary higher-frequency edge resulting from sources at $z < 0.2$. The latter component is dependent on the rate of low-z events, which manifest as time-dependent fluctuations in the higher-frequency edge, showing up because of the inverse-square luminosity distance dependance.

Also apparent during this intermediate period are smaller magnitude non-stationary peaks in the 400 – 700 Hz band as N increases — a result of the small sample space. As the spectrum continues to evolve we see a gradual broadening in bandwidth and smoothing of non-stationary features. The spectrum converges to a broad 200 – 700 Hz monotonically decreasing band from sources in the intermediate range 4 – 0.4 of z. For spectra with $N \geq 10^5$, the high-frequency edge is averaged out. For $N \geq 10^7$, the spectrum converges to the limiting stationary spectral shape shown in Figure 2.

To demonstrate the motion of a PEH we simulate, as a function of observation time, NS birth throughout the Universe. We obtain the running minimum redshift as a function of observation time and convert these to luminosity distances. Figure. 5 plots this data along with a PEH curve representing the 95% probability of an event to occur. Of the 103 events, only one is at a distance greater than the PEH.

6 Discussion and further work

We have investigated the fast temporal evolution of a GW spectrum from a cosmological population of transient sources using a Monte Carlo simulation. We would expect the final spectrum to be biased towards higher frequencies for a SFR model that peaks at a lower z than the SH model used here, although the timescale and form of the temporal evolution is uncertain. For this reason, we plan to extend our work to investigate the evolution of the GW spectrum using other SFR models.

In this initial study, we have employed a highly idealized quasi-monochromatic GW source waveform. We intend to use more realistic waveforms to investigate the dependence of the evolution of the spectrum on the choice of source model. Even with more realistic model waveforms, it is plausible that there are dominant frequencies for each waveform type that will characterize the temporally evolving spectrum.

This study investigates the fast temporal evolution of the spectrum over short observation times, rather than the detectibility of the simulated GW background. Nonetheless, the spectral evolution over long enough observation times has important implications for the detection of transient cosmological GW sources. Advanced GW interferometric detectors will most likely detect the rarer nearby sources, which manifest as the high-frequency edge (see Fig. 3) in our simulations. To determine specific detection strategies and investigate the potential detectability of the events comprising this part of the spectrum will require extending the simulation time. These detection methods will be different from the standard cross-correlation procedure for the frequent high-z events. We plan to investigate parallel signal processing algorithms that encompass events at both high and low z.

The spectral evolution observed in the simulations occurs because of the PEH. It is based on the *act* of observation, where the observer is at the centre of a Universe defined in terms of an event probability distribution. The temporal evolution of the PEH for a particular class of cosmological transient event is defined by the history of event rates. Different types of events,

for example NS births and GRBs, will have different PEH velocities because their mean event rate densities differ, even if both are locked to the SFR. This means the GW spectral evolution from a cosmic population of GW sources depends fundamentally on the source rate history.

Acknowledgments

This research is supported by the Australian Research Council Discovery Grant DP0346344 and is part of the research program of the Australian Consortium for Interferometric Gravitational Astronomy (ACIGA). David Coward is supported by an Australian Postdoctoral Fellowship. We thank Dr André B. Fletcher (Shanghai Astronomical Observatory) for discussions and a careful reading of the manuscript.

References

1. Bennett C *et al* 2003 *Astrophys. J. Suppl.* **148** 1
2. Bunker A, Stanway E, Ellis R and McMahon R 2004 *Preprint* astro-ph/0403223 v2
3. Coward D and Burman R 2004 *submitted to Mon. Not. R. Astron. Soc.*
4. Coward D, Burman R and Blair D 2001 *Mon. Not. R. Astron. Soc.* **324** 1015
5. Coward D, Burman R and Blair D 2002 *Mon. Not. R. Astron. Soc.* **329** 411 (CBB)
6. Dimmelmeier H, Font J and Müller E 2002 *Astron. Astrophys.* **393** 523 (DFM)
7. Ferrari V, Matarrese S and Schneider R 1999 *Mon. Not. R. Astron. Soc.* **303** 247
8. Flanagan É and Hughes S 1998 *Phys. Rev. D.* **57** 4535
9. Fryer C, Holz D and Hughes S 2002 *Astrophys. J.* **565** 430
10. Fryer C, Holz D and Hughes S 2004 *Preprint* astro-ph/0403188 v1 Accepted by *Astrophys. J.*
11. Hernquist L and Springel V 2003 *Mon. Not. R. Astron. Soc.* **341** 1253
12. Howell E, Coward D, Burman R, Blair D and Gilmore J 2004a *Mon. Not. R. Astron. Soc.* **351** 1237
13. Howell E, Coward D, Burman R, Blair D and Gilmore J 2004b *Class. Quantum. Grav.* **21** S551
14. Kotake K, Yamada S, Sato K, Sumiyoshi K, Ono H and Suzuki H 2004 *Phys. Rev. D.* **69** 124004
15. Madau P, Della Valle M and Panagia N 1998 *Astrophys. J.* **297** L17
16. Madau P, Pozetti L and Dickenson A 1998 *Astrophys. J.* **498** 106
17. Miller M, Gressman P and Suen W 2004 *Phys. Rev. D.* **69** 064026
18. Müller E, Rampp M, Buras R, Janka H and Shoemaker 2004 *Astrophys. J.* **603** 221
19. Porciani C and Madau P 2001 *Astrophys. J.* **548** 522
20. Springel V and Hernquist L 2003 *Mon. Not. R. Astron. Soc.* **339** 312 (SH)
21. Yungelson L and Livio M 2000, *Astrophys. J.* **528** 108
22. Zwerger T and Müller E 1997 *Astron. Astrophys.* **320** 209

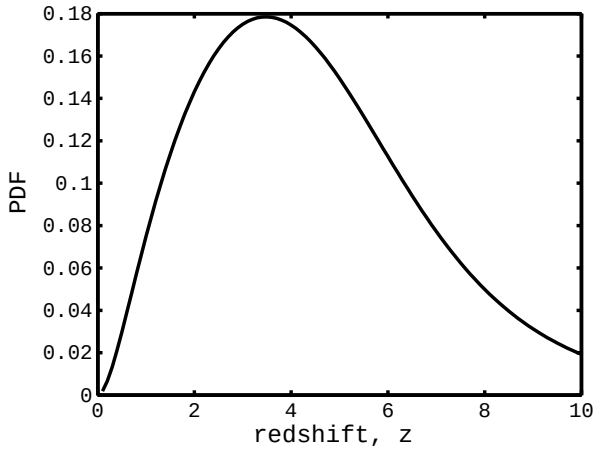

Figure 1: The probability density function for NS births as a function of redshift, based on the SFR model of Hernquist & Springle (2003) in a 'flat-Λ' cosmology.

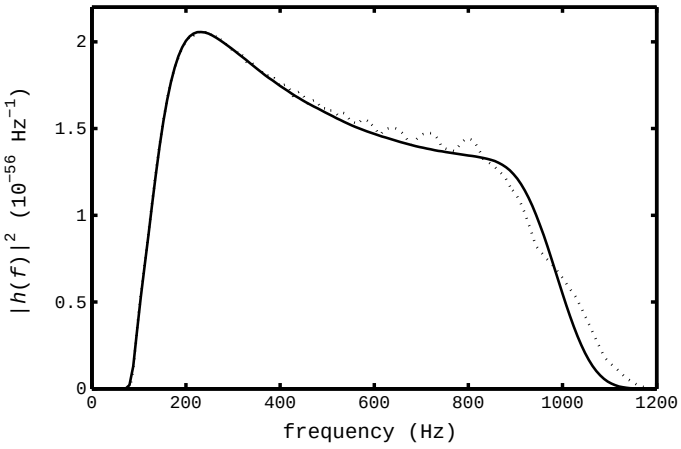

Figure 2: The power spectrum of the GW background as a function of observational frequency for 30 million simulated events, calculated by averaging FFTs of length 2048 (solid line). For comparison, the power spectrum obtained by a convolution of the single-source spectrum with the differential rate, integrated over redshift, is also shown (dotted line); this has been scaled to the maximum magnitude of the simulated spectrum. The oscillations are numerical noise. The peak at just beyond 200 Hz corresponds to the maximum of the differential rate of source formation (Fig. 1).

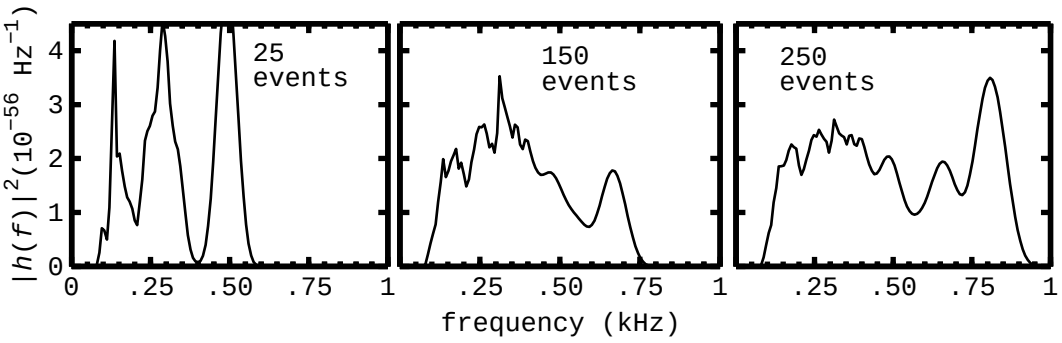

Figure 3: The initial rapid evolution of the GW power spectrum for the first 250 events, equivalent to a time series duration of about 10 s. The first panel shows a bandwidth of about 450 Hz for the first 25 events, equivalent to the first second of the time series. The second and third panels show that significant increases in bandwidth towards higher frequencies occur over the first few hundred events, a result of events occurring at lower redshift.

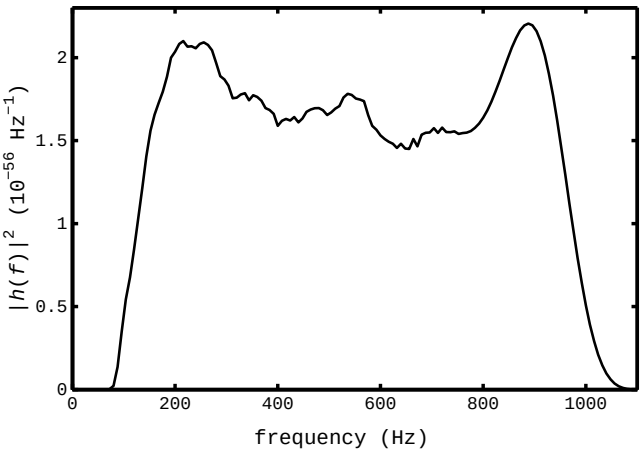

Figure 4: The power spectrum for 10,000 simulated events, corresponding to a time series of about 400-s duration. This period of intermediate temporal evolution is characterized by a broad peak at about 250 Hz, corresponding to the maximum of the differential rate, and a higher-frequency edge from events in the redshift shell $z = 0.002$ to 0.2.

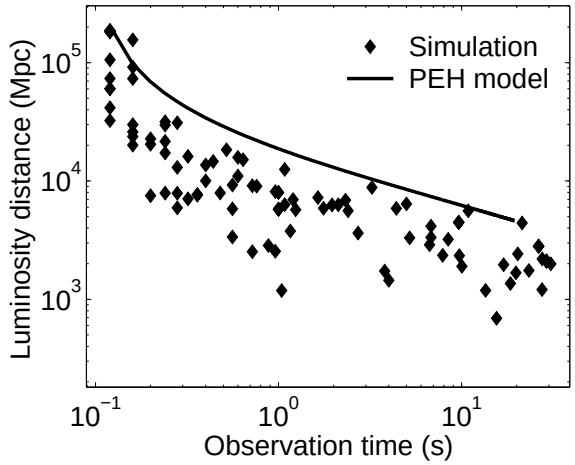

Figure 5: Simulation illustrating the rapid motion of the PEH for the first few tens of seconds of observation time, and a model curve with a probability threshold of 0.95 for at least one event to occur at a distance less than that of the PEH. We assume a universal cumulative event rate of about 25 s^{-1} as seen in our frame, comparable to the NS birth rate integrated throughout the Universe.